

## New Caged Coumarin Fluorophores with Extraordinary Uncaging Cross Sections Suitable for Biological Imaging Applications

YuRui Zhao,<sup>†</sup> Quan Zheng,<sup>†,‡</sup> Kenneth Dakin,<sup>†</sup> Ke Xu,<sup>†</sup> Manuel L. Martinez,<sup>§</sup> and Wen-Hong Li<sup>\*,†</sup>

*Contribution from the Departments of Cell Biology and Biochemistry and Physiology, University of Texas Southwestern Medical Center at Dallas, Dallas, Texas 75390, and Department of Polymer Science and Engineering, University of Science and Technology of China, Hefei, Anhui, P. R. China*

Received June 28, 2003; E-mail: wen-hong.li@utsouthwestern.edu

**Abstract:** Photocaged fluorescent molecules are important research tools for tracking molecular dynamics with high spatiotemporal resolution in biological systems. We have designed and synthesized a new class of caged coumarin fluorophores. These coumarin cages displayed more than 200-fold fluorescence enhancement after UV photolysis. Remarkably, the uncaging cross section of a 1-(2-nitrophenyl)ethyl (NPE)-caged coumarin is 6600 at wavelength of 365 nm, about 2 orders of magnitude higher than previously described caged fluorophores. Product analysis of the photolytic reaction showed clean conversion of NPE-caged coumarin to 2-nitrosoacetophenone and the parent coumarin, suggesting that the mechanism of the photolysis follows the known photochemical reaction pathway of the 2-nitrobenzyl group. We have also measured the two-photon uncaging cross sections of NPE-caged coumarins **2a** and **5** at 740 nm to be near 1 Goeppert-Mayer (GM). The mechanistic study, together with the two-photon uncaging data, suggested that the coumarin moiety serves as an antenna to enhance the light harvesting efficiency of the coumarin cage and that the photonic energy absorbed by coumarin was utilized efficiently to photolyze the NPE group. Future explorations of this type of "substrate-assisted photolysis" may yield other cages of high uncaging cross sections. For cellular imaging applications, we prepared a cell permeable and caged coumarin fluorophore, NPE-HCCC2/AM (**10**), which can be loaded into fully intact cells to high concentrations. Initial tests of this probe in a number of cultured mammalian cells showed desired properties for the in vivo imaging applications. The combined advantages of robust fluorescence contrast enhancement, remarkably high uncaging cross sections, noninvasive cellular delivery, and flexible chemistry for bioconjugations should generate broad applications of these caged coumarins in biochemical and biological research.

### 1. Introduction

Photocaged fluorescent dyes have wide applications in tracking the spatiotemporal dynamics of molecular movements in biological systems.<sup>1–4</sup> These caged tracers are weakly or nonfluorescent when key functional groups of fluorophores are masked by photolabile protecting groups (cages). Photoactivation with ultraviolet (UV) light removes the protecting group (uncage) and abruptly switches on the fluorescence of parent dyes.

Desired properties of caged fluorophores for cellular imaging applications should include high uncaging cross sections, robust fluorescence enhancement after uncaging, and flexible chemistry for bioconjugation and cellular delivery. The uncaging cross section measures the efficiency of photolysis. It equals the product of the quantum yield of uncaging ( $Q_u$ ) and the extinction coefficient ( $\epsilon$ ) of the molecule at the wavelength of photolysis (preferably above 350 nm for imaging applications in live cells using common optics). Thus far the reported caged fluorophores have uncaging cross sections on the order of a hundred when photolyzed at 350 nm or above.<sup>5</sup> New caged fluorescent molecules with higher uncaging cross sections are desirable because we can efficiently turn on their fluorescence while minimizing side effects of UV illumination on live specimens.

Another key requirement for caged fluorophores is that parent fluorophores should be reasonably photostable to resist photo-

<sup>†</sup> Departments of Cell Biology and of Biochemistry, University of Texas Southwestern Medical Center at Dallas.

<sup>‡</sup> University of Science and Technology of China.

<sup>§</sup> Department of Physiology, University of Texas Southwestern Medical Center at Dallas.

(1) Adams, S. R.; Tsien, R. Y. *Annu. Rev. Physiol.* **1993**, *55*, 755.

(2) Politz, J. C. *Trends Cell Biol.* **1999**, *9*, 284.

(3) Kao, J. P. Y.; Adams, S. R. In *Optical Microscopy: Emerging Methods and Applications*; Herman, B., Lemasters, J. J., Eds.; Academic Press: San Diego, CA, 1993; p 27.

(4) Mitchison, T. J.; Sawin, K. E.; Theriot, J. A.; Gee, K.; Mallavarapu, A. *Methods Enzymol.* **1998**, *291*, 63.

(5) Krafft, G. A.; Sutton, W. R.; Cummings, R. T. *J. Am. Chem. Soc.* **1988**, *110*, 301.

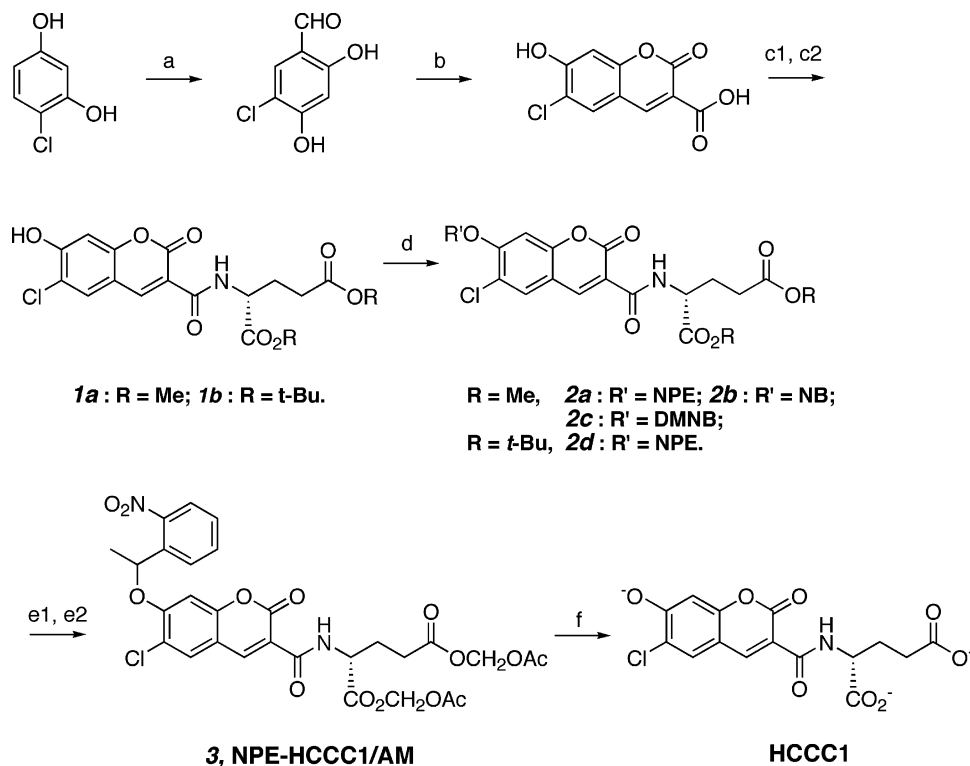


**Figure 1.** Design and syntheses of caged coumarins. (a)  $\text{Zn}(\text{CN})_2$ ,  $\text{HCl}(\text{g})$ ,  $\text{Et}_2\text{O}$ ,  $0^\circ\text{C}$ , and then  $\text{Et}_2\text{O}$ ,  $\text{H}_2\text{O}$ ,  $100^\circ\text{C}$ , 22%. (b) Malonic acid, aniline (cat), pyridine, 44%. (c) (1)  $\text{SOCl}_2$ , cat DMF,  $\text{CH}_2\text{Cl}_2$ . (2) *H*-D-Glu(OMe)-OMe (for **1a**) or *H*-D-Glu(O*t*Bu)-O*t*Bu (for **1b**), TEA,  $\text{CH}_2\text{Cl}_2$ , 67%. (d) NPE bromide (for **2a,d**) or NB bromide (for **2b**) or DMNB bromide (for **2c**), DIEA,  $\text{CH}_2\text{Cl}_2$ , ~65–75%. (e) (1) **2d**, TFA,  $\text{Et}_3\text{SiH}$ ,  $\text{CH}_2\text{Cl}_2$ . (2)  $\text{AcOCH}_2\text{Br}$ , DIEA,  $\text{CH}_3\text{CN}$ , 60%. (f) Hydrolysis by cell esterases and UV uncaging.

bleaching. A major drawback of existing caged fluorophores such as caged fluorescein<sup>5</sup> or caged resorufin<sup>6</sup> is the rapid photobleaching of parent dyes after photoactivation.<sup>4</sup> Photobleaching introduces uncertainties in the fluorescence quantification and makes it difficult to image labeled cells repeatedly over a period of time. In addition, highly reactive oxygen species that are toxic to cells are generated during photobleaching. Rhodamines are less prone to photobleaching than fluorescein or resorufin, and caged rhodamines were subsequently developed to circumvent the problem.<sup>4,7</sup> The uncaging quantum yields of these caged rhodamines have not been reported yet, but they were probably comparable to or less than those of caged fluoresceins.<sup>4</sup> Moreover, since two caging groups were used to protect one rhodamine molecule as bis-carbamates, the efficiency of photolysis was further reduced because both caging groups need to be photolyzed in order to generate one fluorescent molecule. Finally, to apply caged fluorophores to cell imaging, it would be desirable to devise delivery strategies to load these probes inside cells to sufficient concentrations. None of the previously reported caged fluorophores have been derivatized into cell permeable forms that can be enriched inside cells to high concentrations noninvasively.

We now report a new class of caged coumarin fluorophores with very high uncaging cross sections at 365 nm. These caged coumarins exhibit more than 200-fold fluorescence enhancement after photoconversion. In addition, the two-photon uncaging cross sections of two NPE-caged coumarins **2a** and **5** approach 1 Goepfert-Mayer (GM) at 740 nm. To our knowledge, this represents the first example that caged molecules based on an

NPE group can be efficiently photolyzed with infrared light illumination. We have also designed and synthesized a cell permeable derivative of a coumarin cage, NPE-HCCC2/AM, that can be loaded into cells noninvasively. Cellular imaging of this probe demonstrated a combination of advantages.

## 2. Results and Discussion

### 2.1. Design and Syntheses of Caged Coumarins.

We developed a new caged fluorophore based on 6-chloro-7-hydroxy-coumarin 3-carboxamide (**1** of Figure 1) because of its combined advantages including high fluorescence quantum yield, strong absorption above 400 nm, and insensitivity to physiological pH fluctuations.<sup>8</sup> Starting from 4-chloro-resorcinol, we prepared 6-chloro-7-hydroxy-coumarin 3-carboxylate in two steps. Coupling coumarin 3-carboxylate with the methyl ester of D-glutamate provided coumarin 3-carboxamide (**1a**, Figure 1). The dye absorbs maximally at 408 nm with an extinction coefficient of 44 000. The fluorescent quantum yield of the molecule is 0.93 measured in an aqueous buffer (100 mM KCl, 20 mM Mops, pH 7.35). Three caged derivatives of this fluorophore were synthesized by masking the 7-hydroxyl group of coumarin with different cages: 1-(2-nitrophenyl)ethyl (NPE, **2a**, Figure 1), 2-nitrobenzyl (NB, **2b**), and 4,5-dimethoxy-2-nitrobenzyl (DMNB, **2c**) groups.

### 2.2. Photochemical and Fluorescent Properties of Caged Coumarins.

The absorption maxima of all three coumarin cages center around 360 nm (Figure 2A). The absorption spectra also contain broad shoulders between 370 and 380 nm. All three caged coumarins are essentially nonfluorescent, shown by their

(6) Theriot, J. A.; Mitchison, T. J. *Nature* **1991**, 352, 126.

(7) Ottl, J.; Gabriel, D.; Marriott, G. *Bioconjugate Chem.* **1998**, 9, 143.

(8) Zlokarnik, G.; Negulescu, P. A.; Knapp, T. E.; Mere, L.; Burres, N.; Feng, L.; Whitney, M.; Roemer, K.; Tsien, R. Y. *Science* **1998**, 279, 84.

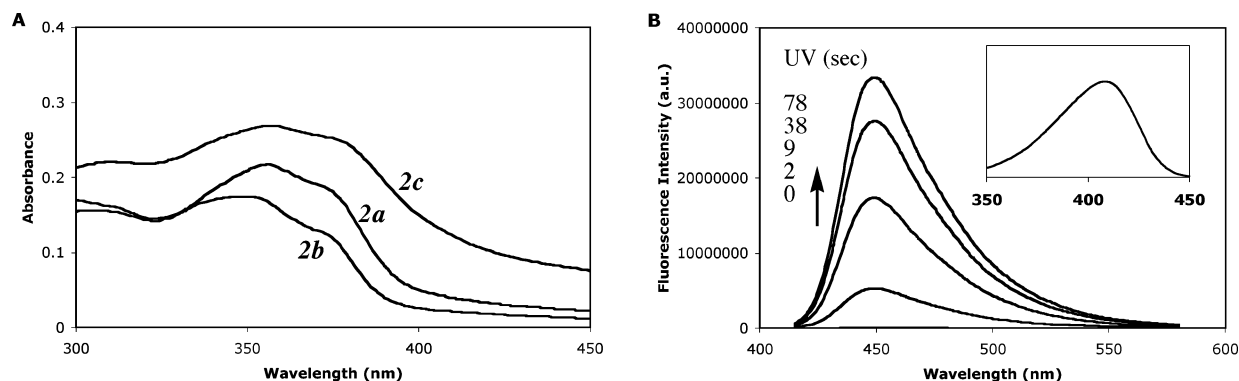


**Figure 2.** (A) Absorption spectra of caged coumarins **2a–c** ( $10 \mu\text{M}$ ). (B) Emission spectra ( $E_x = 410 \text{ nm}$ ) of **2a** ( $1 \mu\text{M}$ ) prior to UV exposure and after increasing durations of UV illuminations. The inset is the excitation spectrum ( $E_m = 450 \text{ nm}$ ) of the exhaustive photolysis product of **2a**. All spectra were taken in 20 mM Mops buffer with 100 mM KCl, pH 7.3.

**Table 1.** Fluorescent and Photochemical Properties of Caged Coumarins<sup>a</sup>

	<b>2a</b>	<b>2b</b>	<b>2c</b>
Caged Coumarins			
$Q_F$	0.0025	0.0048	0.0012
$Q_{F1}/Q_F$	372	194	775
$Q_u^{365 \text{ nm}}$	$0.33 \pm 0.003$	$0.04 \pm 0.004$	$0.0036 \pm 0.0005$
$\epsilon^{365 \text{ nm}}$	20,000	14,000	26,000
$Q_u \epsilon$	6600	560	94

<sup>a</sup>  $Q_F$ : fluorescence quantum yields of caged coumarins.  $Q_{F1}$ : fluorescence quantum yield (0.93) of coumarin **1a**.  $Q_{F1}/Q_F$ : folds of fluorescence enhancement after photoconverting **2a–c** to **1a**. All measurements were done in 20 mM Mops buffer containing 100 mM KCl, pH 7.3.

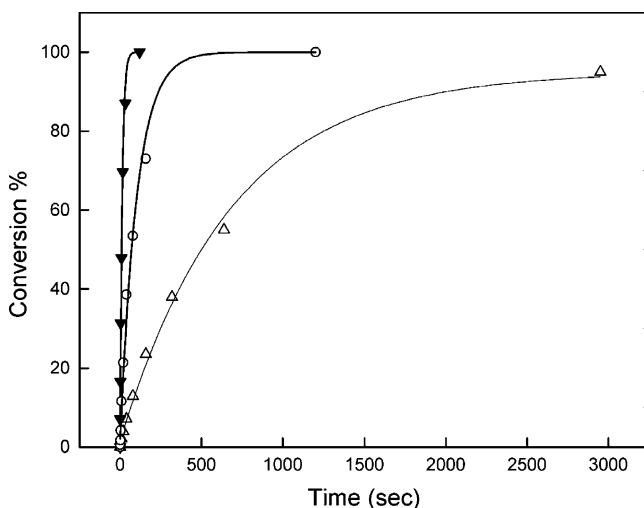


**Figure 3.** Time course of the photoconversion of caged coumarins **2a** (▼), **2b** (○), and **2c** (Δ) to 6-chloro-7-hydroxy-coumarin 3-carboxamide. Caged coumarins ( $\sim 1\text{--}2 \mu\text{M}$  in 20 mM Mops buffer with 100 mM KCl, pH 7.3) illuminated with 365 nm light for various durations. The peak fluorescence emission at 448 nm was measured after each episode of UV illumination and normalized against the fluorescence intensity of a standard of **1a**.

negligible fluorescence quantum yields (Table 1). UV illumination (365 nm) removed the caging group and progressively generated fluorescent products (Figures 2B and 3). The excitation and emission spectra of the exhaustive photolyzed products of three coumarin cages were identical, and they showed no difference from those of coumarin 3-carboxamide **1a**, suggesting

that photoconversion of caged coumarins **2a–c** produced parent coumarin 3-carboxamide **1a**. Further confirmation on the identity of photolysis products came from the high-pressure liquid chromatography (HPLC) analysis (vide infra). The fluorescence enhancements after uncaging ranged from 200-fold (**2b**) to nearly 800-fold (**2c**) (Table 1). This robust change in fluorescence quantum yields is important for generating high contrast optical signals with minimal background.

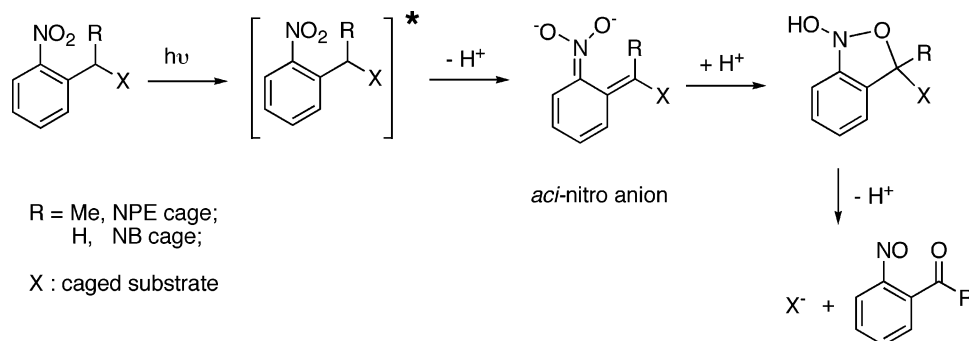
The extent of photoconversion of caged coumarins to coumarin 3-carboxamide depended on the length of UV illumination. NPE-caged coumarin **2a** reached 100% conversion much faster than the other two coumarin cages (Figure 3). The quantum yields of photolysis (determined by the ferrioxalate actinometry)<sup>9</sup> and the uncaging cross sections of three caged fluorophores were measured and are shown in Table 1. There are remarkable differences in the uncaging cross sections among three caged coumarins. The uncaging cross section of NPE-caged coumarin (**2a**) exceeded 6000, about 2 orders of magnitude higher than a previously reported NB-caged fluorescein monoether ( $Q_u \epsilon = 76$  at 350 nm).<sup>5</sup> The NB-caged coumarin (**2b**) has an uncaging cross section significantly lower than that of **2a**, but is still 6 times higher than that of the DMNB caged coumarin (**2c**) or nearly 1 order of magnitude higher than that of a caged fluorescein.<sup>5</sup>

The very high uncaging cross sections of **2a** and **2b** mainly resulted from much increased UV absorption. The extinction coefficients of NB and NPE groups by themselves are less than  $400 \text{ M}^{-1} \text{ cm}^{-1}$  above 360 nm. The theoretical up limits of their uncaging cross sections should be no more than  $400 \text{ M}^{-1} \text{ cm}^{-1}$  above 360 nm even when  $Q_u$  approaches unity. When these caging groups are attached to the 7-hydroxyl group of coumarin, the overall absorbance of the molecule increased by more than 50 times at UV wavelengths. This suggested that the photonic energy absorbed by the coumarin moiety was utilized to photolyze caging groups quite efficiently, at least for the NPE cage **2a** with  $Q_u$  of 33%.

**2.3. Mechanistic Studies of Photolysis of NPE-Caged Coumarins.** The exceptional uncaging efficiency of NPE-caged coumarin **2a** prompted us to investigate the mechanism of its photolysis and to examine the specific roles of NPE group and coumarin moiety in the photochemical reaction. The mechanism of photolysis of 2-nitrobenzyl groups such as NB or NPE groups has been thoroughly studied.<sup>10–13</sup> Upon UV excitation, 2-ni-

(9) Hatchard, C. G.; Parker, C. A. *Proc. R. Acad. London A* **1956**, *235*, 518.

## Scheme 1



trobenzyl group or substituted versions such as an NPE group forms an *aci*-nitro intermediate either through a singlet or a triplet excited state (Scheme 1). Once formed, the *aci*-nitro intermediate decays to generate the parent substrate and 2-nitroso benzaldehyde (from NB) or 2-nitrosoacetophenone (from NPE).

If the photolysis of NPE-caged coumarin **2a** proceeds according to the above mechanism, it should generate two products: 2-nitrosoacetophenone and coumarin **1a**. Figure 4 shows HPLC analyses of the product formation after photolyzing NPE-caged coumarin **2a** and 1-(2-nitrophenyl)ethyl acetate (NPE acetate). We included NPE acetate in the photolysis study to calibrate the elution time of 2-nitrosoacetophenone on the HPLC chromatogram. After UV illumination, the peak corresponding to NPE acetate (peak 1, Figure 4A) decreased. This change was accompanied by the formation of a new peak with an earlier elution time at 4.3 min (peak 2, Figure 4A). The absorption maximum of NPE acetate is 262 nm (spectrum 1, Figure 4B). The absorption spectrum of the exhaustively photolyzed solution containing NPE acetate (spectrum 2, Figure 4B) showed the absorption maximum at 280 nm with a shoulder at 315 nm. This spectrum is identical with the absorption spectrum of peak 2 of trace b in Figure 4A (data not shown), and it is in excellent agreement with the reported absorption spectrum of 2-nitrosoacetophenone.<sup>14</sup> Thus, we assigned peak 2 of Figure 4A eluting at 4.3 min as 2-nitrosoacetophenone.

Figure 4C shows HPLC chromatograms of NPE-caged coumarin **2a** and its photolysis products. The chromatograms were displayed by taking the absorbance at 310 nm to show the caged coumarin **2a** (peak 3, Figure 4C) and two photolyzed products (peaks 2 and 4, Figure 4C) on the same chromatogram with comparable peak heights. The HPLC chromatogram of the synthesized coumarin **1a** (trace d, Figure 4C) was also listed as a reference. Prior to UV illumination, NPE-caged coumarin **2a** was eluted off the column after 9.2 min (trace a, peak 3 of Figure 4C). After UV photolysis (trace b, Figure 4C), peak 3 decreased, and two new peaks appeared at 2.2 min (peak 2) and 4.3 min (peak 4), respectively. Peak 2 of Figure 4C was identified as 2-nitrosoacetophenone because its elution time (4.3 min) and absorption spectrum are the same as those of peak 2 in Figure 4A. Peak 4 corresponded to the synthesized coumarin **1a** because it showed the same elution time (2.2 min), absorption, excitation, and emission spectra (data not shown). The identity

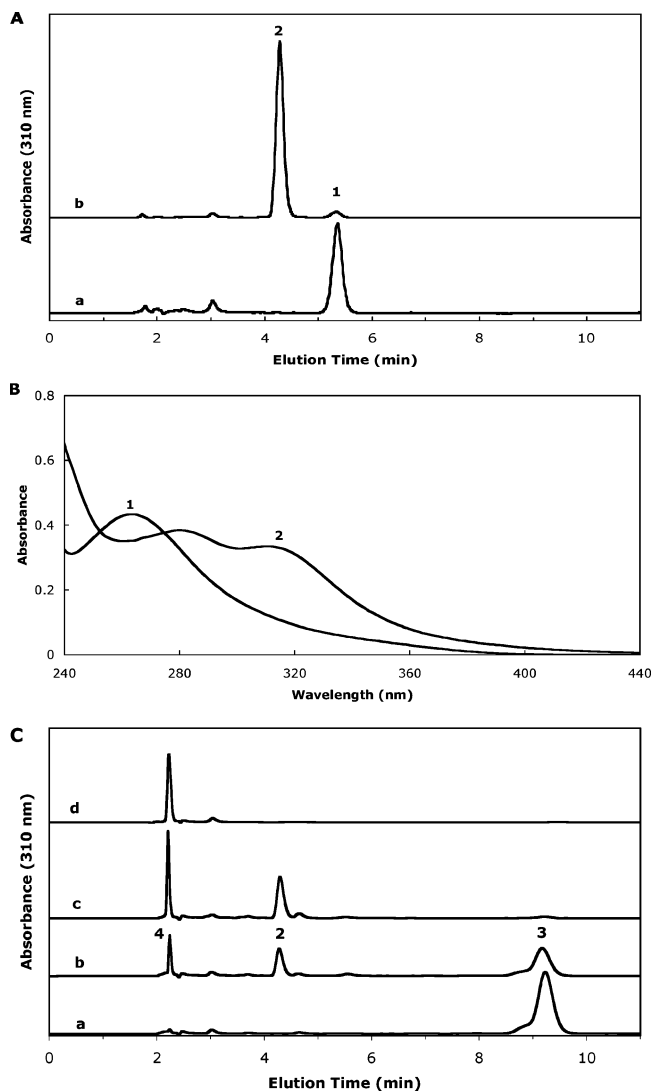


**Figure 4.** HPLC analysis of the photolysis products. (A) Chromatograms of NPE acetate before (trace a) and after (trace b) UV illumination (365 nm, 1000 s). The absorbance of trace b was scaled down 3 times relative to trace a. (B) Absorption spectra of NPE acetate (90  $\mu$ M) before (1) and after (2) UV illumination. (C) Chromatograms of NPE-caged coumarin **2a** before (trace a) and after photolysis at 365 nm (trace b, 50 s UV; and trace c, 200 s UV). Trace d is the chromatogram of the synthesized coumarin **1a**. The minor left shoulder of peak 3 is believed to be a stereoisomer of compound **2a**. All samples were eluted with an isocratic mixture of 70% acetonitrile and 30% water at a flow rate of 1 mL/min.

of the product in peak 4 was further confirmed by mass spectroscopy analysis, which showed the expected molecular weight peak at 397.86 ( $[M + H]^+$ , 397.06 calcd for coumarin

(10) McCray, J. A.; Trentham, D. R. *Annu. Rev. Biophys. Biophys. Chem.* **1989**, *18*, 239.

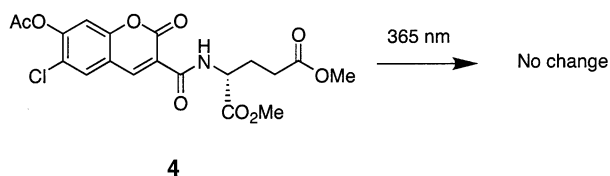
(11) Corrie, J. E.; Barth, A.; Munasinghe, V. R.; Trentham, D. R.; Hutter, M. *C. J. Am. Chem. Soc.* **2003**, *125*, 8546.

(12) Schupp, H.; Wong, W. K.; Schnabel, W. *J. Photochem.* **1987**, *36*, 85.

(13) Zhu, Q. Q.; Schnabel, W.; Schupp, H. *J. Photochem.* **1987**, *39*, 317.

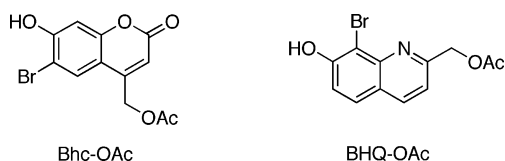
(14) Walker, J. W.; McCray, J. A.; Hess, G. P. *Biochemistry* **1986**, *25*, 1799.

Scheme 2



**1a** of formula  $C_{17}H_{16}ClNO_8$ ). Longer UV illumination completed the photoconversion of caged coumarin **2a** to 2-nitroacetophenone and free coumarin 3-carboxamide **1a** (trace c, Figure 4C).

The above product studies confirmed photolytic decomposition of NPE-caged coumarin **2a** to the expected products based on the known mechanism of photochemical reaction of 2-nitrobenzyl groups. Recently, 6-bromo-7-hydroxycoumarin-4-ylmethyl (Bhc) and analogous groups have been developed as photolabile protecting groups mainly for two-photon uncaging applications.<sup>15</sup> In addition, Dore and co-workers have reported the synthesis and photochemistry of 8-bromo-7-hydroxyquinoline-2-ylmethyl (BHQ) group and its applications in photocaging.<sup>16</sup> The one-photon uncaging cross sections of these cages range from several hundreds to slightly over a thousand at 365 nm.

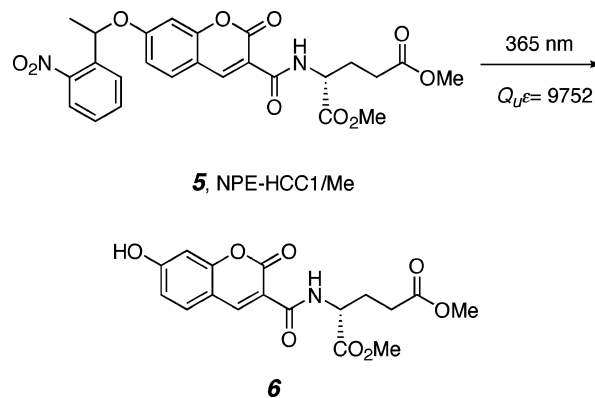


Both the Bhc group and our NPE-caged coumarin **2a** share a coumarin structural core. However, NPE-caged coumarin **2a** reported here is distinguished from Bhc or analogous groups in at least two major aspects. First, in our system, 6-chloro-7-hydroxy coumarin 3-carboxamide was the fluorescent substrate that was caged by an NPE group, whereas Bhc, BHQ, or related groups were designed as photolabile protecting groups for caging other molecules. Unlike Bhc or BHQ group, 6-chloro-7-hydroxy coumarin 3-carboxamide such as **1a** is fairly resistant to UV illumination. In addition, continuous illumination of 6-chloro-7-acetoxy-coumarin 3-carboxamide (**4** of Scheme 2) with 365 nm UV light over 5 min had little effect on the integrity of the molecule as shown by the HPLC analysis (Figure S1, Supporting Information). This further suggested that 6-chloro-7-hydroxy-coumarin 3-carboxamide by itself is inert to UV light, at least under the same condition where NPE-caged coumarin **2a** was completely photolyzed.

Second, the mechanism of photolytic cleavage of coumarin-4-ylmethyl group has been postulated to be a photo  $S_N1$  reaction, and a coumarinylmethyl cation intermediate has been suggested based on  $^{18}O$  labeling experiments.<sup>17</sup> In contrast, the mechanism of photochemical reaction in our system involves the classical 2-nitrobenzyl photolysis as inferred from the HPLC and spectroscopic analyses.

During the photolysis of caged coumarin **2a**, the coumarin moiety most likely plays an “antenna” role by transferring

Scheme 3



energy to the NPE group after absorbing UV light. This greatly enhances the overall uncaging efficiency of the coumarin cage. Since 6-chloro substituent is next to the photocleavage site, we examined whether chlorine substitution at the 6-position of coumarin is necessary for the “coumarin-assisted photolysis”. To address the question, we prepared an NPE-caged 7-hydroxycoumarin 3-carboxamide (NPE-HCC1/Me, compound **5**, Scheme 3). The compound has an even more impressive uncaging quantum yield of 0.53 at 365 nm ( $\epsilon^{365nm} = 18\,400$ ,  $Q_U = 9752$ , measured in pH 7.3 Mops buffer), about 60% higher than the NPE-caged coumarin **2a**. Product analysis by HPLC after photolyzing **5** also confirmed expected photolytic reaction generating 2-nitroacetophenone and parent 7-hydroxy coumarin 3-carboxamide **6** based on the known mechanism of the NPE group (Figure S2, Supporting Information). The increase in  $Q_U$  after removing 6-chlorine substitution probably reflected a decrease in steric hindrance between the NPE group and coumarin moiety so that NPE group may adopt more favorable conformations for receiving photonic energy from coumarin. In addition, chlorine substitution should have effects on intersystem crossing or on the relative rates of excited-state decay, etc. These variations may also affect the efficiency of photolysis. Further studies would be required to address the issue.

These examples showed that caged substrates can dramatically improve the efficiency of photolysis of caging groups by enhancing the absorption of UV light. Future explorations of this type of “substrate-assisted photolysis” may yield other cages of high uncaging cross sections. Since the NPE group by itself has fairly weak absorption above 350 nm, it is unlikely that the photonic energy absorbed by the coumarin moiety was transferred to the NPE group mainly through the Förster’s type of dipole coupling. An alternative pathway is that the NPE group and the coumarin moiety are strongly coupled to form a “semiconjugated chromophore” in which excitation is delocalized over caged coumarin **2a**. Support for this hypothesis came from the comparison of the absorption spectra of 6-chloro-7-methoxy-coumarin 3-carboxamide and NPE-caged coumarin **2a**.

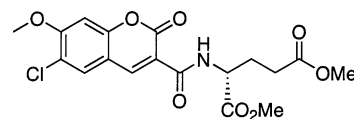
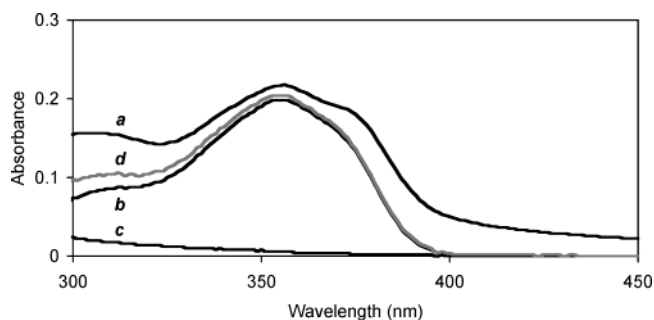


Figure 5 shows that the “composite spectrum” (trace d, Figure 5) of equimolar 1-(2-nitrophenyl)ethanol and 6-chloro-7-methoxy-

(15) Furuta, T.; Wang, S. S.; Dantzker, J. L.; Dore, T. M.; Bybee, W. J.; Callaway, E. M.; Denk, W.; Tsien, R. Y. *Proc. Natl. Acad. Sci. U.S.A.* **1999**, *96*, 1193.

(16) Fedoryak, O. D.; Dore, T. M. *Org. Lett.* **2002**, *4*, 3419.

(17) Schade, B.; Hagen, V.; Schmidt, R.; Herbrich, R.; Krause, E.; Eckardt, T.; Bendig, J. *J. Org. Chem.* **1999**, *64*, 9109.



**Figure 5.** Absorption spectra of NPE-caged coumarin **2a** (trace a), 6-chloro-7-methoxy-coumarin 3-carboxamide (trace b), and 1-(2-nitrophenyl)ethanol (trace c). All three spectra were taken in 20 mM Mops buffer (pH 7.3) containing 10  $\mu$ M substrate. The composite spectrum of equimolar 1-(2-nitrophenyl)ethanol and 6-chloro-7-methoxy-coumarin 3-carboxamide is represented by trace d.

oxy-coumarin 3-carboxamide nearly overlapped with the measured spectrum of 6-chloro-7-methoxy-coumarin 3-carboxamide (trace b). The spectra (traces b and d) showed fairly low absorbance above 400 nm. In contrast, the UV-vis spectrum of caged coumarin **2a** (trace a) showed much stronger absorption above 400 nm, and the absorbance of caged coumarin **2a** is higher than the “composite spectrum” (trace d) throughout. This probably indicates that there is a sizable coupling between the NPE group and the coumarin moiety in **2a**. The coupling probably also exists in the NB- and DMNB-caged coumarins (compounds **2b** and **2c**, Figure 1) as indicated by the similarity of the absorption spectra of three caged fluorophores (Figure 2A). However, the photonic energy absorbed by the coupled chromophore was utilized to photolyze three caging groups with quite different efficiencies (Table 1). The order of uncaging quantum yields among caged coumarins **2a–c** is consistent with the general observation made in many other caged molecules: for the same caged substrate, the NPE cage usually has the highest uncaging quantum yield, whereas the DMNB cage is photolyzed least efficiently.<sup>3,5</sup>

**2.4. Two-Photon Uncaging of NPE-Caged Coumarins.** A recent development in the photouncaging field was the introduction of the two-photon uncaging technique.<sup>15,18–20</sup> This method involves applying high fluxes of infrared (IR) laser light to excite samples in a highly restricted focal volume,  $\sim 1 \mu\text{m}^3$ . Simultaneous absorptions of two or more IR photons with a combined energy equivalent to one UV photon pump the molecule to the excited states. By comparison with the usual one-photon UV photolysis, two-photon uncaging offers the advantages of releasing active molecules with excellent three-dimensional resolution and minimizing photo toxicity to cells. The efficiency of two-photon photolysis is measured as the two-photon uncaging action cross section,  $\delta_u$ . This parameter is the product of the two-photon absorbance cross section,  $\delta_a$ , and the uncaging quantum yield,  $Q_{u2}$ , and is measured in the unit of Goeppert-Mayer (1 GM =  $10^{-50} \text{cm}^4 \cdot \text{s}/\text{photon}$ ).<sup>15,18</sup> Ideally,  $\delta_u$  of caged molecules should exceed 0.1 GM for biological applications in live specimens.<sup>15</sup>

Tsien and co-workers first developed Bhc as a two-photon cage of general usages.<sup>15</sup> More recently, Dore and co-workers described using BHC as another protecting group of sufficient

sensitivity for the two-photon photolysis.<sup>16</sup> These newly developed caging groups have been used to protect carboxylates,<sup>15,16</sup> phosphates,<sup>17,19,21</sup> diols,<sup>22</sup> aldehydes, and ketones.<sup>23</sup> Molecules caged by these groups display two-photon uncaging cross sections about 1 GM at 740 nm. In addition, 4-methoxy-7-nitroindoline (MNI) group has also been applied as a two-photon caging group, though the  $\delta_u$  (0.06 GM at 730 nm) of a MNI-caged glutamate is significantly lower than those of molecules based on Bhc or BHC groups.<sup>20,24</sup>

In contrast to these recent developments, caged compounds employing 2-nitrobenzyl or related protecting groups have fairly low  $\delta_u$ . DMNB-caged compounds such as DM-nitrophen and DMNB-acetate have  $\delta_u$  of  $\sim 0.01–0.03$  GM between 720 and 740 nm. Other caged molecules based on NB or NPE groups have negligible  $\delta_u$ .<sup>15,18</sup> Since our mechanistic studies on the photolytic reaction of NPE-caged coumarin indicated energy coupling between coumarin 3-carboxamide and the nearby NPE caging group, and because 7-hydroxycoumarin and analogous chromophores have relatively high two-photon absorption cross sections,<sup>15,25</sup> we proceeded to investigate the sensitivity of NPE-caged coumarins **2a** and **5** (NPE-HCC1/Me, Scheme 3) toward two-photon photolysis.

To calculate  $\delta_u$ , we used 6-bromo-7-hydroxycoumarin-4-ylmethyl acetate (Bhc-OAc) as a reference compound.<sup>15,16</sup> Bhc-OAc and caged coumarins **2a** or **5** in microcuvettes were illuminated using focused infrared light (740 nm) from a femtosecond-pulsed and mode-locked Ti:sapphire laser. The two-photon uncaging action cross section can be determined using the equation:<sup>15</sup>

$$\delta_u = \frac{2N_p}{C_s \langle I_0^2(t) \rangle \int S^2(r) dV} \quad (1)$$

where  $N_p$  is the number of product molecules formed per unit time,  $\langle I_0^2(t) \rangle$  is the mean squared light intensity,  $S(r)$  is a unitless spatial distribution function, the integral is over the volume of the microcuvette, and  $C_s$  is the substrate concentration. If caged compounds are photolyzed under the identical setting with the same two-photon laser power, then the term  $\langle I_0^2(t) \rangle \int S^2(r) dV$  should be about the same for different cages. Thus,  $\delta_u^a$  of cage a can be determined by comparing its rate of product formation ( $N_p^a$ ) with that of reference cage b with known  $\delta_u^b$  according to the equation:

$$\frac{\delta_u^a}{\delta_u^b} = \frac{N_p^a C_s^b}{N_p^b C_s^a} \quad (2)$$

The formation of coumarins after two-photon photolysis of **2a** and **5** was quantified similarly as in the one-photon uncaging experiments by measuring the fluorescence enhancement. The photolysis of Bhc-OAc was quantified by HPLC analysis as described.<sup>15,16</sup> Figure 6 shows time courses of the photolysis of Bhc-OAc and NPE-caged coumarins **2a** and **5**. Both caged

(20) Matsuzaki, M.; Ellis-Davies, G. C.; Nemoto, T.; Miyashita, Y.; Iino, M.; Kasai, H. *Nat. Neurosci.* **2001**, *4*, 1086.

(21) Furuta, T.; Iwamura, M. *Methods Enzymol.* **1998**, *291*, 50.

(22) Lin, W.; Lawrence, D. S. *J. Org. Chem.* **2002**, *67*, 2723.

(23) Lu, M.; Fedoryak, O. D.; Moister, B. R.; Dore, T. M. *Org. Lett.* **2003**, *5*, 2119.

(24) Caneparri, M.; Nelson, L.; Papageorgiou, G.; Corrie, J. E.; Ogden, D. J. *Neurosci. Methods* **2001**, *112*, 29.

(25) Parma, L.; Omenetto, N. *Chem. Phys. Lett.* **1978**, *54*, 541.

(18) Brown, E. B.; Shear, J. B.; Adams, S. R.; Tsien, R. Y.; Webb, W. W. *Biophys. J.* **1999**, *76*, 489.

(19) Ando, H.; Furuta, T.; Tsien, R. Y.; Okamoto, H. *Nat. Genet.* **2001**, *28*, 317.

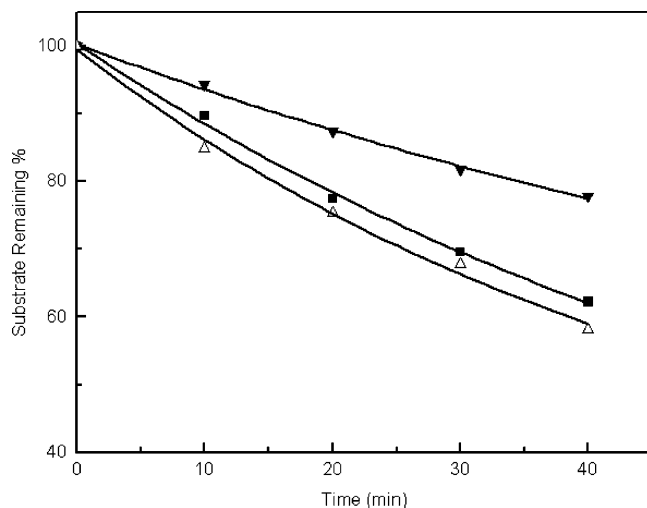


**Figure 6.** Time course of two-photon uncaging of NPE-caged coumarin **2a** ( $\nabla$ ), **5** ( $\blacksquare$ ), and Bhc-OAc ( $\triangle$ ) at 740 nm (average power 590 mW exiting the cuvette). The formation of coumarin **1a** from **2a** (initial concentration 10  $\mu$ M) was measured by fluorescence spectroscopy. The photolysis of Bhc-OAc (initial concentration 100  $\mu$ M) was followed by HPLC. Solid lines are least-squares fits of simple decaying exponentials.

coumarins **2a**, **5**, and Bhc-OAc were photolyzed by 740-nm laser light quite efficiently, yet Bhc-OAc and **5** were about two times more sensitive to two-photon uncaging than **2a**. Since the reported  $\delta_u$  of Bhc-OAc has been measured at 740 nm at the laser power of 345 mW exiting the cuvette,<sup>16</sup> we also compared the rates of photolysis of **2a**, **5**, and Bhc-OAc at this power level. After 20 min of continuous illumination, 5.5, 10, and 10.6% of photolysis occurred for compounds **2a**, **5**, and Bhc-OAc, respectively. Using the reported  $\delta_u$  of Bhc-OAc (0.72 GM at 740 nm)<sup>15,16</sup> and eq 2, we estimated  $\delta_u$  of **2a** and **5** to be 0.37 and 0.68 GM, respectively. In addition, product analysis by HPLC after two-photon photolysis of caged coumarins **2a** and **5** showed the same chromatograms as those obtained after one-photon uncaging (data not shown), suggesting that the NPE group was converted to 2-nitrosoacetophone efficiently after two-photon illuminations.

Thus far caged compounds employing NPE or NB groups have shown unmeasurably low two-photon uncaging action cross sections. To our knowledge, our newly developed NPE-caged coumarins such as **2a** and **5** represented the first example that  $\delta_u$  of caged compounds based on 2-nitrobenzyl groups can approach 1 GM. This result further supported our proposed mechanism that the coumarin moiety serves as an antenna to enhance the light harvesting capability of the molecule and to boost the photolytic efficiency of NPE group.

**2.5. Caged and Cell Permeable Coumarins for in Vivo Fluorescence Imaging Applications.** To apply these caged coumarins for imaging applications in live cells, we attempted to derivatize them into cell membrane permeant forms. We focused our initial efforts on NPE-caged coumarin 3-carboxamide such as **2a** because of its combined advantages, including high uncaging cross sections and robust fluorescence enhancement after uncaging. In addition, its parent fluorophore 7-hydroxy-6-chloro-coumarin-3-carboxamide (HCCC1, Figure 1) is relatively insensitive to physiological pH fluctuations. We first attempted to protect two carboxylates of D-glutamate of **2a** with acetoxymethyl (AM) esters (compound **3**, Figure 1). AM esters are stable in physiological solutions but are susceptible to

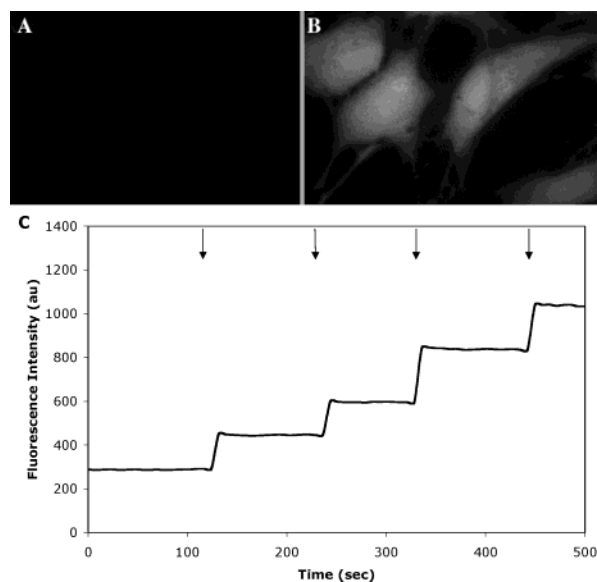


**Figure 7.** Fluorescence imaging of HeLa cells loaded with a caged and cell permeable coumarin **3**. HeLa cells were loaded with 2  $\mu$ M **3** for 1 h in the Hanks balanced salt solution (HBSS, pH 7.35) containing 10 mM Hepes buffer and 5.5 mM glucose. After washing, cells on glass coverslips were imaged on an inverted microscope (Axiovert 200, Carl Zeiss). During the imaging, cells were briefly illuminated with UV light (330–380 nm), indicated by the arrows in part C. The first two arrows denote 0.1 s UV exposures, and the last two arrows represent 0.2 s UV. (A and B) Fluorescent images of cells before and after UV uncaging, respectively. (C) Average fluorescence intensity of cells in the field of view over the course of four episodes of UV photolysis.

hydrolysis by cellular esterases. The enzymatic hydrolysis regenerates negatively charged carboxylates which are trapped inside cells.<sup>26</sup> Initial attempts of hydrolyzing two methyl esters of **2a** under a number of conditions were accompanied by the concomitant hydrolysis of the amide bond of coumarin 3-carboxamide. Instead, we found that protecting two carboxylates of glutamate with *tert*-butyl groups provided a more feasible synthetic route. Thus, acid treatments of the intermediate **2d** (prepared from **1b**, Figure 1) followed by esterification with AM bromide afforded the AM ester of NPE-caged coumarin **3** (NPE-HCCC1/AM, Figure 1).

Figure 7 shows fluorescence images of HeLa cells loaded with coumarin cage **3**. Fluorescent imaging was taken by using excitation bandpass filters with cut-on wavelength longer than 420 nm. Prior to uncaging, continuous monitoring of cells loaded with **3** showed that there was no difference in fluorescence intensity of loaded cells from control cells, indicating that the background fluorescence of coumarin cage is negligible (Figure 7A). Subsequent UV illumination generated a sudden jump of cellular blue fluorescence (Figure 7B), and repetitive uncaging caused stepwise increases of coumarin fluorescence (Figure 7C).

To test if NPE-HCCC1/AM performs the same as a fluorescent marker in other types of cells, we further evaluated its fluorescence imaging properties in different cell lines. After loading and uncaging of NPE-HCCC1/AM in cultured primary human fibroblasts, we noticed that the coumarin fluorescence in these cells was not as stable as that in HeLa cells. Figure 8A shows that the coumarin fluorescence intensity of HCCC1 gradually decayed in primary fibroblasts after whole field uncaging.

(26) Li, W. H.; Llopis, J.; Whitney, M.; Zlokarnik, G.; Tsien, R. Y. *Nature* **1998**, *392*, 936.

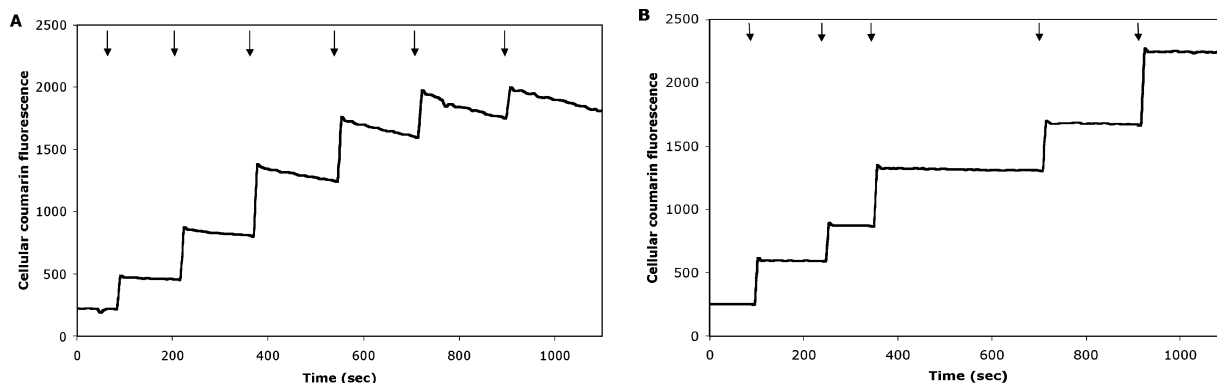


**Figure 8.** Fluorescence signal of HCCC1 (A) is less stable than that of HCCC2 (B) in primary human fibroblasts. Human primary fibroblasts were loaded with caged coumarin NPE-HCCC1/AM (A) or NPE-HCCC2/AM (B), imaged, and uncaged similarly as in Figure 7. Arrows indicate UV flashes of various durations (seconds): 0.2, 0.4, 0.8, 1.2, 1.6, and 2 (from left to right) (A) and 0.2, 0.2, 0.4, 0.4, and 0.8 (B).

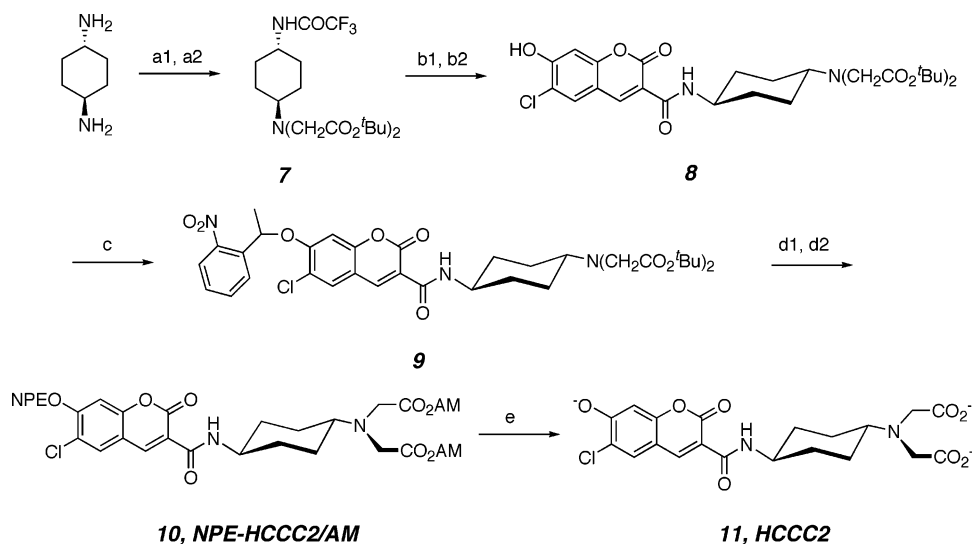


**Figure 9.** Synthesis of a caged and cell permeable coumarin, NPE-HCCC2/AM. (a) (1) Trifluoroacetic anhydride,  $\text{CH}_2\text{Cl}_2$ , r.t., (2)  $\text{BrCH}_2\text{CO}_2^t\text{Bu}$ ,  $\text{KHCO}_3$ , DMF, 36% for two steps. (b) (1) 1 N NaOH, THF, (2) 6-Chloro-7-hydroxy-coumarin 3-carboxylate,  $\text{SOCl}_2$ , cat DMF,  $\text{CH}_2\text{Cl}_2$ ,  $\text{Et}_3\text{N}$ , 24% for two steps. (c) NPE bromide, DIEA,  $\text{CH}_2\text{Cl}_2$ , 57%. (d) (1) TFA,  $\text{Et}_3\text{SiH}$ ,  $\text{CH}_2\text{Cl}_2$ , (2)  $\text{BrCH}_2\text{OAc}$ , DIEA,  $\text{CH}_2\text{Cl}_2$ , 33% for two steps. (e) Hydrolysis by cell esterases and UV uncaging.

The decline of fluorescence signal of HCCC1 was also observed in a few other cell lines tested, such as COS cells and NIH3T3 fibroblasts, yet the rates of its intensity decay were slower than what was observed in primary fibroblasts. At the moment we are not yet clear about the causes for the gradual loss in coumarin fluorescence intensity, though we speculated that it might be due to a slow metabolism of 7-hydroxy-6-chloro-coumarin 3-carboxamide (HCCC1, Figure 1) in these cells.

To improve the fluorescence signal stability of coumarin 3-carboxamide in cells, we designed a new coumarin fluorophore HCCC2 (**11**, Figure 9) in which 1,4-*cis*-diaminocyclohexane *N,N*-diacetate was conjugated with coumarin 3-carboxylate. We reasoned that increasing steric hindrance of the amide bond of coumarin 3-carboxamide should enhance its enzymatic stability. In addition, incorporating *N,N*-diiminoacetates moiety in the molecule should improve its cellular retention. The synthesis of its caged and cell permeable precursor NPE-HCCC2/AM (**10**) is shown in Figure 9.

To our satisfaction, caged coumarin NPE-HCCC2/AM loaded quite well into cells. Repetitive photouncaging generated stepwise increases in cell coumarin fluorescence, which remained stable in primary fibroblasts (Figure 8B). We also tested the compound in other types of cultured mammalian cells,

including HeLa cells, NIH3T3 fibroblasts, COS cells, CHO cells, and 1321N1 astrocytoma cells. In all these cells, the compound showed essentially the same desired imaging properties, including ease of loading, high sensitivity toward UV photolysis, and stability of coumarin fluorescence signal after uncaging. Thus, NPE-HCCC2/AM is of more general utility as a fluorescent marker in mammalian cells than NPE-HCCC1/AM.

In summary, we have designed and synthesized a new class of caged coumarins suitable for *in vivo* imaging applications. By comparison with previous caged fluorophores, our newly developed caged coumarins show a number of advantages, including photostability of parent dyes, high uncaging efficiency, and much improved cell loading properties. Since the coumarins described here emit blue light, they spectrally complement many existing fluorescent sensors emitting at green or red regions. The combinatory uses of these coumarin cages with other fluorescent dyes or indicators which emit at longer wavelengths may allow us to expand the fluorescent imaging window and to carry out photouncaging and multicolor imaging simultaneously in live cells. Since NPE-caged coumarins such as **2a** and **5** possess high two-photon uncaging action cross sections, this class of caged coumarins may also have applications in biological systems where the two photon uncaging technique



is preferred to UV photolysis. Finally, the synthetic strategy outlined in Figure 1 would allow assembling other derivatives of these caged coumarins by conjugating coumarin 3-carboxylate with various amines. This provides a facile route of introducing different reactive groups into the molecule for the bioconjugation. The syntheses of these derivatives and their applications in biological imaging are in progress and will be reported in due course.

### 3. Experimental Section

**3.1. Materials and General Methods.** All reagents were purchased from Aldrich or Fluka. Anhydrous solvents for organic syntheses were purchased from Aldrich and stored over activated molecular sieves (4 Å). Thin-layer chromatography (TLC) was performed on precoated silica gel 60F-254 glass plates. Reaction products were purified by low-pressure flash chromatography (FC) using silica gel 60 (~63–200  $\mu\text{m}$ , EM Science). Syntheses of caged compounds sensitive to near-UV light were carried out in an isolated room equipped with red safety lamps.  $^1\text{H}$  NMR spectra were obtained using Varian 300 or 400 MHz spectrometers. Chemical shifts ( $\delta$ , ppm) were reported against TMS (0 ppm). MALDI-TOF mass spectroscopy was performed on a Voyager-DE PRO biospectrometry workstation (Applied Biosystems) using 2,5-dihydroxy benzoic acid as the matrix. UV-vis spectra were recorded in a 1-cm path quartz cell on a Shimadzu 2401 PC spectrometer. Fluorescence excitation and emission spectra were recorded on a Fluorolog 3 spectrometer (Jobin-Yvon Horiba, Edison, NJ). Bhc-OAc was synthesized as described.<sup>15</sup>

**3.2. Syntheses. 2,4-Dihydroxy-5-chlorobenzaldehyde.** The compound was synthesized from 4-chlororesorcinol using a previously described procedure.<sup>27</sup>  $^1\text{H}$  NMR ( $\text{CDCl}_3$ ,  $\delta$  ppm): 11.25 (s, 1H), 9.69 (s, 1H), 7.52 (s, 1H), 6.62 (s, 1H), 6.18 (br s, 1H).

**6-Chloro-7-hydroxy-coumarin 3-Carboxylate.** A suspension of the above benzaldehyde (0.58 g, 3.36 mmol), malonic acid (0.72 g, 6.9 mmol), and a catalytic amount of aniline in pyridine (3.0 mL) was stirred at room temperature (rt) for 72 h. EtOH (5.0 mL) was then added. The mixture was stirred at this temperature for 1 h and filtered. The filtrate was washed sequentially with 0.1 N HCl,  $\text{H}_2\text{O}$ , and  $\text{Et}_2\text{O}$  to afford a yellow solid. The solid was dried under high vacuum overnight to give the desired product as a yellow powder (0.35 g, 43.7%).  $^1\text{H}$  NMR ( $\text{DMSO}-d_6$ ,  $\delta$  ppm): 8.62 (s, 1H), 7.96 (s, 1H), 6.87 (s, 1H). MS: 239.98 calcd for  $\text{C}_{10}\text{H}_5\text{ClO}_5$ ; obsd: 241.47 (M + H)<sup>+</sup>, 263.47 (M + Na)<sup>+</sup>, 279.45 (M + K)<sup>+</sup>.

**6-Chloro-7-hydroxy-coumarin 3-Carboxamide (1b).** A droplet of DMF was added to a suspension of 6-chloro-7-hydroxy-coumarin 3-carboxylate (85 mg, 0.35 mmol) and  $\text{SOCl}_2$  (0.253 mL, 3.477 mmol) in  $\text{CH}_2\text{Cl}_2$  (5.0 mL). The mixture was stirred at 45 °C for 4 h and then evaporated to dryness. The residue was resuspended in 2 mL dry  $\text{CH}_2\text{Cl}_2$ . To this suspension a solution of *H*-D-di-*tert*-butyl glutamate hydrogen chloride (157 mg, 0.53 mmol) and  $\text{Et}_3\text{N}$  (196  $\mu\text{L}$ , 1.4 mmol) in  $\text{CH}_2\text{Cl}_2$  (3.0 mL) was added. The resulting mixture was stirred at rt overnight. The solution was then poured into EtOAc, extracted with 0.1 N HCl, washed with brine, dried over  $\text{Na}_2\text{SO}_4$ , and concentrated to a residue. The residue was purified by FC ( $\text{CH}_2\text{Cl}_2/\text{MeOH}$ , 95:5) to afford **1b** as a pale yellow powder (89 mg, 52.6%).  $^1\text{H}$  NMR ( $\text{CDCl}_3$ ,  $\delta$  ppm): 9.24 (d,  $J = 8.0$  Hz, 1H), 8.65 (s, 1H), 7.56 (s, 1H), 6.98 (s, 1H), 4.64 (m, 1H), 2.31–2.42 (m, 2H), 2.18–2.28 (m, 2H), 1.47 (s, 9H), 1.41 (s, 9H). MS: 481.15 calcd for  $\text{C}_{23}\text{H}_{28}\text{ClNO}_8$ ; obsd: 504.70 (M + Na)<sup>+</sup>, 520.67 (M + K)<sup>+</sup>.

Compound **1a** was synthesized similarly from *H*-D-dimethyl glutamate hydrogen chloride. **1a**:  $^1\text{H}$  NMR ( $\text{CDCl}_3$ ,  $\delta$  ppm): 9.17 (d,  $J = 7.6$  Hz, 1H), 8.71 (s, 1H), 7.64 (s, 1H), 7.04 (s, 1H), 4.79 (m, 1H), 3.78 (s, 3H), 3.67 (s, 3H), 2.4–2.5 (m, 2H), 2.15–2.40 (m, 2H). MS: 397.06

calcd for  $\text{C}_{17}\text{H}_{16}\text{ClNO}_8$ ; obsd: 398.59 (M + H)<sup>+</sup>, 420.56 (M + Na)<sup>+</sup>, 436.54 (M + K)<sup>+</sup>.

**6-Chloro-7-[1-(2-nitrophenyl)ethoxy]-coumarin 3-Carboxamide (2d).** A solution of **1b** (45.3 mg, 94  $\mu\text{mol}$ ), NPE bromide (25.9 mg, 0.113 mmol), and DIEA (32.7  $\mu\text{L}$ , 0.187 mmol) in acetonitrile (300  $\mu\text{L}$ ) was stirred at 45 °C for 10 h. After cooling, the reaction mixture was directly purified by silica gel chromatography with  $\text{CH}_2\text{Cl}_2/\text{MeOH}$  (98:2) as eluant. The desired product was obtained as a solid after drying (42.8 mg, 72.5%).  $^1\text{H}$  NMR ( $\text{CD}_3\text{Cl}$ ,  $\delta$  ppm): 9.05 (d,  $J = 8.0$  Hz, 1H), 8.66 (s, 1H), 8.05 (d,  $J = 8.0$  Hz, 1H), 7.58–7.72 (m, 3H), 7.45 (m, 1H), 6.67 (d,  $J = 1.6$  Hz, 1H), 6.22 (q,  $J = 6.4$  Hz, 1H), 4.62 (m, 1H), 2.13–2.34 (m, 4H), 1.76 (d,  $J = 6.0$  Hz, 3H), 1.43 (s, 9H), 1.36 (s, 9H). MS: 630.20 calcd for  $\text{C}_{31}\text{H}_{35}\text{ClN}_2\text{O}_{10}$ ; obsd: 653.99 (M + Na)<sup>+</sup>, 669.97 (M + K)<sup>+</sup>.

Compounds **2a–c** were synthesized similarly as **2d** from **1a**.

**2a**:  $^1\text{H}$  NMR ( $\text{CD}_3\text{Cl}$ ,  $\delta$  ppm): 9.08 (d,  $J = 8.0$  Hz, 1H), 8.69 (s, 1H), 8.10 (d,  $J = 8.0$  Hz, 1H), 7.6–7.75 (m, 3H), 7.4–7.5 (m, 1H), 6.71 (d,  $J = 2.0$  Hz, 1H), 6.27 (q,  $J = 6.4$  Hz, 1H), 4.78 (m, 1H), 3.76 (d, 3H), 3.64 (d, 3H), 2.23–2.5 (m, 3H), 2.03–2.18 (m, 1H), 1.80 (d,  $J = 6.1$  Hz, 3H). MS: 546.10 calcd for  $\text{C}_{25}\text{H}_{23}\text{ClN}_2\text{O}_{10}$ ; obsd: 569.8 (M + Na)<sup>+</sup>, 585.82 (M + K)<sup>+</sup>.

**2b**:  $^1\text{H}$  NMR ( $\text{CD}_3\text{Cl}$ ,  $\delta$  ppm): 9.14 (d,  $J = 7.6$  Hz, 1H), 8.76 (s, 1H), 8.25 (dd,  $J = 8.4$ , 1H), 8.00 (d,  $J = 8.2$  Hz, 1H), 7.76 (t,  $J = 7.6$ , 1H), 7.72 (s, 1H), 7.57 (t,  $J = 7.6$  Hz, 1H), 7.05 (s, 1H), 5.62 (s, 2H), 4.80 (m, 1H), 3.77 (s, 3H), 3.67 (s, 3H), 2.3–2.5 (m, 3H), 2.08–2.18 (m, 1H). MS: 532.09 calcd for  $\text{C}_{24}\text{H}_{21}\text{ClN}_2\text{O}_{10}$ ; obsd: 533.94 (M + H)<sup>+</sup>, 555.89 (M + Na)<sup>+</sup>, 571.88 (M + K)<sup>+</sup>.

**2c**:  $^1\text{H}$  NMR ( $\text{CD}_3\text{Cl}$ ,  $\delta$  ppm): 9.14 (d,  $J = 7.6$  Hz, 1H), 8.76 (s, 1H), 7.81 (s, 1H), 7.75 (s, 1H), 7.6 (s, 1H), 7.12 (s, 1H), 5.62 (s, 2H), 4.80 (m, 1H), 4.05 (s, 3H), 3.98 (s, 3H), 3.77 (s, 3H), 3.65 (s, 3H), 2.3–2.52 (m, 3H), 2.08–2.18 (m, 1H). MS: 592.11 calcd for  $\text{C}_{26}\text{H}_{25}\text{ClN}_2\text{O}_{12}$ ; obsd: 593.69 (M + H)<sup>+</sup>, 615.69 (M + Na)<sup>+</sup>, 631.67 (M + K)<sup>+</sup>.

**NPE-HCCCI/AM (3)**: A solution of **2d** (12 mg, 0.0191 mmol),  $\text{CF}_3\text{CO}_2\text{H}$  (38.4  $\mu\text{L}$ , 0.498 mmol), triethylsilane (7.5  $\mu\text{L}$ , 0.048 mmol), and  $\text{CH}_2\text{Cl}_2$  (100  $\mu\text{L}$ ) was stirred at rt. The reaction was continued until two *tert*-butyl esters were completely hydrolyzed, as monitored by TLC. The reaction mixture was concentrated under high vacuum and used directly for the esterification. After being dried, the resulting residue was resuspended in acetonitrile (200  $\mu\text{L}$ ). Bromomethyl acetate (3.5  $\mu\text{L}$ , 0.0466 mmol) and DIEA (11.1  $\mu\text{L}$ , 0.636 mmol) were then added. The mixture was left at rt overnight. After the solvent was removed, water (200  $\mu\text{L}$ ) was added. The mixture was extracted with  $\text{CH}_2\text{Cl}_2$  (3  $\times$  10 mL). The combined extracts were dried ( $\text{Na}_2\text{SO}_4$ ) and concentrated. The residue was purified by flash chromatography eluting with  $\text{CH}_2\text{Cl}_2/\text{MeOH}$  (98/2) to give 6.3 mg of desired product (60%).  $^1\text{H}$  NMR ( $\text{CD}_3\text{Cl}$ ,  $\delta$  ppm): 9.09 (d,  $J = 7.6$  Hz, 1H), 8.68 (s, 1H), 8.11 (d,  $J = 8.0$  Hz, 1H), 7.6–7.8 (m, 3H), 7.49 (m, 1H), 6.71 (s, 1H), 6.27 (m, 1H), 5.69–5.81 (m, 4H), 4.79 (m, 1H), 2.55–2.52 (m, 2H), 2.31–2.40 (m, 2H), 2.11 (s, 3H), 2.09 (s, 3H), 1.81 (d,  $J = 6.4$  Hz, 3H). MS: 662.12 calcd for  $\text{C}_{29}\text{H}_{27}\text{ClN}_2\text{O}_{14}$ ; obsd: 663.86 (M + H)<sup>+</sup>, 685.86 (M + Na)<sup>+</sup>.

***N,N*-di-*tert*-butylacetate-*N'*-trifluoroacetamide 1,4-*cis*-Diaminocyclohexane (7).** Trifluoroacetic anhydride (0.91 mL, 6.550 mmol) was added to a solution of 1,4-*cis*-diaminocyclohexane (0.68 g, 5.955 mmol) in  $\text{CH}_2\text{Cl}_2$  at 0 °C. The resulting mixture was stirred at rt overnight. It was then diluted with  $\text{CH}_2\text{Cl}_2$ , washed with saturated  $\text{NaHCO}_3$  and brine, and concentrated to give a white solid. This was used directly for the next step without further purification.

The crude monotrifluoroacetamide (0.30 g, 1.427 mmol) obtained above was mixed with  $\text{KHCO}_3$  (0.36 g, 3.596 mmol) in DMF (2.0 mL). *tert*-Butyl bromoacetate (0.47 mL, 3.139 mmol) was added dropwise at rt. The resulting mixture was stirred overnight and then diluted with EtOAc (300 mL), washed with saturated  $\text{NH}_4\text{Cl}$  solution, dried over  $\text{Na}_2\text{SO}_4$ , and concentrated under vacuum. The residue was purified by FC eluted with hexane/EtOAc (9:1 to 4:1) to afford **7** as a colorless oil

(27) Tsien, R. Y.; Zlokarnik, G. U.S. Patent 6,472,205, 2002.

(223 mg, 35.6% for two steps).  $^1\text{H NMR}$  (400 MHz,  $\delta$  ppm,  $\text{CDCl}_3$ ): 6.14 (d,  $J = 7.3$  Hz, 1H), 3.71 (m, 1H), 3.43 (s, 4H), 2.68 (m, 1H), 2.04 (d,  $J = 12.0$  Hz, 2H), 1.94 (d,  $J = 12.0$  Hz, 2H), 1.42 (s, 18H), 1.19–1.38 (m, 4H). MS: 438.23 calcd for  $\text{C}_{20}\text{H}_{33}\text{F}_3\text{N}_2\text{O}_5$ ; obsd: 439.14 ( $\text{M} + \text{H}^+$ ), 461.12 ( $\text{M} + \text{Na}^+$ ).

**6-Chloro-7-hydroxy-coumarin 3-Carboxamide (8).** Monotrifluoroacetamide **7** (75 mg, 0.172 mmol) was saponified with NaOH (171  $\mu\text{L}$ , 1 N) in MeOH (2 mL) overnight. It was then diluted with EtOAc (100 mL), washed with saturated  $\text{NaHCO}_3$ , dried over  $\text{Na}_2\text{SO}_4$ , and concentrated to a residue which was used immediately for the next step.

The above amine was dissolved in 2 mL of  $\text{CH}_2\text{Cl}_2$ . 6-Chloro-7-hydroxycoumarin 3-carbonyl chloride (0.0894 mmol, prepared as in making **1b**) suspended in  $\text{CH}_2\text{Cl}_2$  (2.0 mL) was then added.  $\text{Et}_3\text{N}$  (37.4  $\mu\text{L}$ , 0.274 mmol) was added shortly afterward. The resulting mixture was stirred at rt overnight and then diluted with EtOAc (150 mL), washed with brine, and dried over  $\text{Na}_2\text{SO}_4$ . The concentrated residue was purified by FC (hexane/EtOAc, 3:2 to 1:1) to afford **8** as a yellow solid (12.2 mg, 24% for two steps).  $^1\text{H NMR}$  (400 MHz,  $\delta$  ppm,  $\text{CDCl}_3$ ): 8.74 (s, 1H), 8.62 (d,  $J = 8.0$  Hz, 1H), 7.66 (s, 1H), 7.06 (s, 1H), 3.86 (m, 1H), 3.44 (s, 4H), 2.70 (m, 1H), 2.09 (d,  $J = 10.6$  Hz, 2H), 1.94 (d,  $J = 10.6$  Hz, 2H), 1.45 (s, 18H), 1.24–1.39 (m, 4H). MS: 564.22 calcd for  $\text{C}_{28}\text{H}_{37}\text{ClN}_2\text{O}_8$ ; obsd: 565.87 ( $\text{M} + \text{H}^+$ ), 587.86 ( $\text{M} + \text{Na}^+$ ).

**7-[1-(2-Nitrophenyl)ethoxy]-6-chloro-coumarin 3-Carboxamide (9).** 6-Chloro-7-hydroxy-coumarin 3-carboxamide (**8**, 7.4 mg, 13  $\mu\text{mol}$ ), NPE-Br (4.5 mg, 20  $\mu\text{mol}$ ), and DIEA (6.8  $\mu\text{L}$ , 39  $\mu\text{mol}$ ) were mixed in  $\text{CH}_3\text{CN}-\text{CH}_2\text{Cl}_2$  (0.5 mL, 1:1). The solution was stirred at 40  $^\circ\text{C}$  for 8 h and then cooled. The reaction mixture was diluted with EtOAc (10 mL), washed with saturated  $\text{NH}_4\text{Cl}$  and dried over  $\text{Na}_2\text{SO}_4$ . The concentrated residue was purified by FC eluted with hexane/EtOAc (4:1 to 7:3) to afford NPE-caged coumarin **9** as a slightly yellow solid (5.4 mg, 57.4%).  $^1\text{H NMR}$  (400 MHz,  $\delta$  ppm,  $\text{CDCl}_3$ ): 8.71 (s, 1H), 8.48 (d,  $J = 8.0$  Hz, 1H), 8.10 (dd,  $J = 8.0, 1.0$  Hz, 1H), 7.40–7.78 (m, 4H), 6.69 (s, 1H), 6.25 (q,  $J = 6.4$  Hz, 1H), 3.83 (m, 1H), 3.45 (s, 4H), 2.69 (m, 1H), 2.07 (d,  $J = 10.9$  Hz, 2H), 1.93 (d,  $J = 10.6$  Hz, 2H), 1.80 (d,  $J = 6.4$  Hz, 3H), 1.42 (s, 18H), 1.2–1.43 (m, 4H). MS: 713.27 calcd for  $\text{C}_{36}\text{H}_{44}\text{ClN}_3\text{O}_{10}$ ; obsd: 714.17 ( $\text{M} + \text{H}^+$ ), 736.16 ( $\text{M} + \text{Na}^+$ ).

**NPE-HCCC2/AM (10):** NPE-caged coumarin **9** (5.4 mg, 7.56  $\mu\text{mol}$ ) and triethylsilane (5.9  $\mu\text{L}$ , 38  $\mu\text{mol}$ ) were dissolved in  $\text{CH}_2\text{Cl}_2$  (200  $\mu\text{L}$ ).  $\text{CF}_3\text{CO}_2\text{H}$  (15.7  $\mu\text{L}$ , 0.204 mmol) was added. The resulting solution was stirred at rt in the dark for 4.5 h and then evaporated to a residue. The dried residue was dissolved in acetonitrile (150  $\mu\text{L}$ ). To this solution, bromomethyl acetate (3.7  $\mu\text{L}$ , 38  $\mu\text{mol}$ ) and DIEA (13.2  $\mu\text{L}$ , 76  $\mu\text{mol}$ ) were added. The solution was stirred at rt in the dark overnight, diluted with  $\text{CH}_2\text{Cl}_2$  (10 mL), washed with saturated  $\text{NH}_4\text{Cl}$ , dried over  $\text{Na}_2\text{SO}_4$ , and concentrated. The residue was purified by FC eluting with hexane/EtOAc (3:2) to afford the final product **7** (1.8 mg, 32.5% for two steps) as a yellow solid. MS: 745.19 calcd for  $\text{C}_{34}\text{H}_{36}\text{ClN}_3\text{O}_{14}$ ; obsd: 746.25 ( $\text{M} + \text{H}^+$ ), 768.23 ( $\text{M} + \text{Na}^+$ ).  $^1\text{H NMR}$  (400 MHz,  $\delta$  ppm,  $\text{CDCl}_3$ ): 8.71 (s, 1H), 8.49 (d,  $J = 8.0$  Hz, 1H), 8.10 (dd,  $J = 8.0, 1.2$  Hz, 1H), 7.73 (dd,  $J = 8.0, 1.2$  Hz, 1H), 7.67 (s, 1H), 7.64 (m, 1H), 7.49 (m, 1H), 6.69 (s, 1H), 6.25 (q,  $J = 6.4$  Hz, 1H), 5.75 (s, 4H), 3.82 (m, 1H), 3.62 (s, 4H), 2.71 (m, 1H), 2.04–2.18 (m, 8H), 1.92 (d,  $J = 6.4$  Hz, 2H), 1.80 (d,  $J = 6.4$  Hz, 3H), 1.20–1.42 (m, 4H).

**3.3. Quantum Yields of One-Photon Photolysis.** The one-photon photolysis quantum yields were determined by irradiating  $\sim 1\text{--}2$   $\mu\text{M}$  of caged coumarins in a buffered solution (10 mM Kops, 100 mM KCl, pH 7.3) with 365-nm UV light from a mercury lamp (B-100 AP; UVP, Upland, CA). Durations of UV irradiation were controlled by an electronic shutter (Uniblitz, Vincent Associates, Rochester, NY). After each episode of UV illumination, fluorescence emission spectra of the samples were measured. The excitation wavelength was set at

420 nm or above to minimize photolysis during fluorescence measurements. The percentage of photolysis was calculated from the fluorescence enhancement normalized against the fluorescence intensity of pure 6-chloro-7-hydroxy-coumarin 3-carboxamide (compound **1a**; Figure 1). The progress of photochemical reaction was plotted as simple decaying exponentials. Quantum yields of uncaging ( $Q_u$ ) were calculated from the equation  $Q_u = -\log(C/C_0)/(I\sigma t)$ , where  $I$  is the irradiation intensity in einsteins $\cdot\text{cm}^{-2}\cdot\text{s}^{-1}$ ,  $\sigma$  is the decadic extinction coefficient in  $\text{cm}^2\cdot\text{mol}^{-1}$  ( $10^3$  times of the usual extinction coefficient  $\epsilon$  in  $\text{M}^{-1}\text{cm}^{-1}$ ),  $t$  is the irradiation time in seconds, and  $C$  and  $C_0$  are concentrations of caged coumarins at time  $t$  and at the beginning of photolysis, respectively.<sup>26</sup> The total UV intensity  $I$  was measured with the ferrioxalate actinometry,<sup>9</sup> and it was typically in the range of  $\sim 0.5\text{--}1.02 \times 10^{-8}$  E/( $\text{cm}^2\cdot\text{s}$ ).

**3.4. Product Analysis and Mechanistic Studies of Photolysis of Caged Coumarins.** The photolysis products were analyzed by HPLC. A Shimadzu HPLC system (SCL-10A vp controller) equipped with an auto injector, a photodiode array detector, and a fluorescence detector was used. Separations were carried out on an analytical reverse-phase column (250 mm  $\times$  4.6 mm, Luna C-18/5  $\mu\text{m}$ , Phenomenex, Torrance, CA) using an isocratic flow of  $\text{CH}_3\text{CN}/\text{H}_2\text{O}$  (7:3). Caged coumarins (compounds **2a** or **5**, 70  $\mu\text{M}$ ) in Mops buffer (20 mM Mops, 100 mM KCl, pH 7.3) were photolyzed with 365 nm of light. The sample was then diluted with acetonitrile and analyzed by HPLC. To calibrate the retention time of 2-nitrosoacetophenone, 1-(2-nitrophenyl)ethyl acetate was photolyzed and analyzed by HPLC under the same condition.

**3.5. Measurements of Two-Photon Uncaging Cross Sections.** Two-photon photolysis was carried out using a procedure similar to the one first described by Furuta et al.<sup>15</sup> Samples in 100 mM Mops buffer (pH 7.3) were transferred to a microcuvette (Hellma 105.251-QS). The filling volume of the cuvette was 45  $\mu\text{L}$ . The laser beam from a femtosecond-pulsed and mode-locked Ti:sapphire laser (Mira 900-F pumped by a Verdi, Coherent, Santa Clara, CA) was focused into the center of the cuvette with a focusing lens (01 LPX 029/077, focal length 25 mm, Melles-Griot, Carlsbad, CA). After irradiation with 740 nm of light, samples were collected, and the formation of the products was quantified by measuring fluorescence enhancements or by HPLC analysis. Two-photon uncaging cross sections ( $\delta_u$ ) were calculated from eq 2 using the reported  $\delta_u$  of 0.72 GM for Bhc-OAc at 345 mW laser power exiting the cuvette.<sup>16</sup> Since the percent of photolysis of caged coumarins **2a** and **5** changed little at concentrations 10  $\mu\text{M}$  or above (data not shown), we used 10  $\mu\text{M}$  of **2a** and **5** in the microcuvette during the two-photon photolysis.

**3.6. Uncaging and Fluorescence Imaging of Caged Coumarins in Cultured Cells.** Hela cells were cultured in high glucose DMEM medium (Gibco) containing 10% fetal bovine serum and 1% penicillin/streptomycin. Human primary fibroblasts isolated from foreskin (generously supplied by Dr. Frederick Grinnell) were cultured in the same medium and were used until 20 doublings were reached. Cells to be imaged were cultured on 35-mm Petri dishes with glass bottoms (MatTek, Ashland, MA). Fluorescence microscopy was carried out on an inverted fluorescence microscope (Axiovert 200, Carl Zeiss) with a 40 $\times$  objective. Epifluorescence was detected with a cooled CCD camera (ORCA-ER, Hamamatsu). Cells were excited with light from a 175 W xenon lamp after passing through appropriate bandpath filters. Switching of excitation wavelengths between UV uncaging and image acquisition was controlled by a high-speed wavelength switcher (Lambda DG-4, Sutter Instrument). Image acquisition and analysis were accomplished using an integrated imaging software (Openlab, Improvision).

**Acknowledgment.** This research was supported by a research grant (I-1510) from the Welch Foundation and a Career Development Award from the American Diabetes Associations to W.-h.L. We thank Dr. Helen Yin for generously allowing us

to use her two-photon laser systems. We also thank Dr. Frederick Grinnell for providing primary human fibroblasts.

**Supporting Information Available:** Synthesis of coumarin derivatives and HPLC analysis of photolysis products of **4** and

**5** (PDF). This material is available free of charge via the Internet at <http://pubs.acs.org>.

JA036958M